Preprint, 11th IFAC Symposium on Dynamics and Control of Process Systems,
including Biosystems
June 6-8, 2016. NTNU, Trondheim, Norway

Constrained Multivariable Predictive Control of a Train of Cryogenic ^{13}C Separation Columns

Clara M. Ionescu [*,**] **Cristina I. Muresan** [**] **Dana Copot** [*]
Robin De Keyser [*]

[*] *Ghent University, Department of Energy and Systems, Research Group on Dynamical Systems and Control (DYSC), Technologiepark 914, 2nd floor, Ghent 9052, Belgium (e-mail: claramihaela.ionescu@ugent.be).*
[**] *Technical University of Cluj Napoca, Department of Automation, 2628 Gh. Bariiu Street, room 350, ClujNapoca, Romania (e-mail: cristina.pop@aut.tucluj.ro)*

Abstract: This work presents a linear, constrained, multivariable predictive control strategy, i.e. EPSAC (Extended Prediction Self-Adaptive Control) applied to a train of three distillation columns. The columns are used to obtain the carbon isotope ^{13}C used widely in medicine and specific industries. The oversimplified models of the three columns stem from a real-life plant designed and constructed in the National Institute for Research and Development for Isotopic and Molecular Technologies, in Cluj Napoca, Romania. The simulation results suggest the strategy is applicable to this process.

Keywords: multivariable control, predictive control, constrained control, distillation column, Smith Predictor scheme

1. INTRODUCTION

There are only a few research centres in the world concerned with such isotope separation processes. In Romania the only research center in this domain is the National Institute for Research and Development for Isotopic and Molecular Technologies Cluj-Napoca (NIRDIMT). Here was conceived, designed and built such a separation equipment for the 13C enrichment process, becoming one of the very few European centres or countries where is *produced* this isotope. There is a lack in the literature of papers concerned with the isotope separation processes due to safety and copyright issues. There are no scientific or technological data about the separation column of 13C or works detailing the column control.

Despite the lack of production sites, the 13C carbon isotope plays a significant role in diagnosis of cancer and other organ function monitoring tests (Axente et al., 1994).

One single dedicated equipment can offer 13C isotope enrichment up to (8-10) at%, due to physical limitations (Muntean et al., 2012). However many applications needs higher 13C concentration, up to 90%, which can not be achieved with a single column. Two directions are possible to increase the 13C concentration: to build a higher column or to use more columns *connected* in a cascaded fashion. The first solution has several drawbacks in terms of efficiency, construction, thermal insulation, etc. Neither from economical point of view is not an approved solution, implying higher energy consumption, higher maintenance costs. At NIRDIMT the adopted solution was the construction of a train of three columns of medium height.

The research regarding trains of distillation columns, or more specifically of cryogenic isotope separation columns, is scarce, with a few notable papers (Skogestad, 1997; Luyben, 2013). A train of five distillation columns for the recovery of valuable heavier hydrocarbons from natural gas is presented in (Luyben, 2013). In (Muresan et al., 2015), a multivariable internal model control approach with time delay compensation and decoupling properties has been introduced for the train of distillation columns at NIRDIMT. Triggered by these results, the aim of this paper is to perform a feasibility study whether or not a multivariable, constrained linear model predictive control (MPC) strategy would provide added value with respect to performance, robustness to model uncertainty and time delays. More specifically, we employ here our *in-house* algorithm, the Extended Prediction Self-Adaptive Control (EPSAC) strategy (De Keyser, 2003). The objective is to tailor the control algorithm for the specific dynamics of this exotic process. Robustness to modelling errors are also investigated.

The paper is organized as follows: the next section describes the process and the model used to simulate the process. Third section introduced the EPSAC approach to MPC and fourth section presents the results obtained. A

[⋆] This work is financially supported by a grant of the Romanian National Authority for Scientific Research, CNDI UEFISCDI, project number 155/2012 PN-II-PT-PCCA-2011-3.2-0591.

conclusion section summarizes the main outcome of this work and points out to further developments.

2. DESCRIPTION OF THE PROCESS

The schematic representation of the 13C isotope separation columns built at NIRDIMT is given in Fig. 1, with the main components of one column being: the distillation column, the condenser (C1) at the top of the column cooled with liquid nitrogen, electrical boiler at the bottom of the column and vacuum jacket for thermal isolation, since the column operates at very low temperatures. Carbon monoxide (CO) is fed as a gas through a feeding system, at an intermediary point in the column (Pop et al., 2010; Muntean et al., 2012). Flow transducers (FT) and flow controllers (FC)/pumps are installed on the feed, waste and product flows. A dedicated level transducer (LT) for liquid CO (Patent # RO128052) is also installed at the bottom of the column and a level controller (LC). Pressure transducers (PT) are installed at the top and bottom of the column.

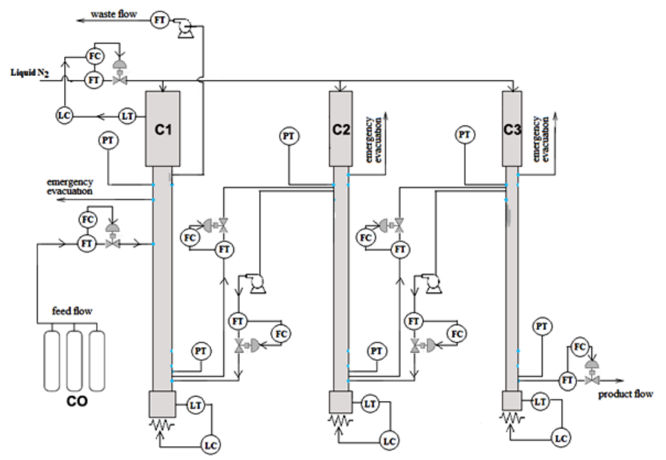

Fig. 1. Schematic of a train of distillation columns.

Since the vapour pressure depends on the temperature, so is the separation coefficient (Bisgaard et al., 2015). At very low temperatures around -196^{o}C - the 12CO vapour pressure is greater than that of 13CO and thus the carbon isotopes can be separated through distillation, with the 12C accumulating in the gaseous phase and the 13C being predominant in the liquid phase (Pop et al., 2010).

For the column to operate efficiently, the top and bottom column pressures need to be maintained at their prescribed set points, as well as the liquid nitrogen level in the condenser and the liquid carbon monoxide level at the boiler. The liquid nitrogen in the condenser represents the main trigger for the low column temperature needed in order to ensure a significant separation coefficient, thus the level needs to be accurately controlled. The liquid carbon monoxide level also plays an important role since it is based on the boiling of this quantity that the two isotopes can be separated. Finally, the pressures in the column play a significant role since they influence the boiling point of the carbon monoxide (Axente et al., 1994; Muresan et al., 2015). The remaining three outputs of the process, the two pressures and the liquid carbon monoxide, will be controlled in a multivariable fashion by manipulating the feed and waste flows, as well as the electrical power supplied to the boiler at the bottom of the column.

Figure 1 presents the schematic of the train of distillation columns. The first column is fed with carbon monoxide at an intermediary point approximately one third from the top of the column. The enriched 13C gas from the bottom of the first column is taken as the feed to the top of the second column, while the enriched 13C gas from the bottom of the second column is fed to the top of the third column. This flow occurs due to the pressure difference that exists between the top and bottom parts of the columns. The waste flow from the third column is extracted at the top and is fed back into the bottom of the second column, while the waste from this second column is fed into the bottom of the first one. This flow is operated using flow controllers and dedicated pumps, as indicated in Figure 1. The waste from the first column is taken outside the train of distillation units, into a special reservoir.

The model of a single 13C isotope separation column, linearized around its equilibrium point and scaled in a [-100%,+100%] range, has been determined previously (Pop et al., 2012). As indicated in Figure 1, each column has a different diameter, however the electrical power supplied to the boiler and the flows that enter/exit the column are scaled to the requirements of each individual column. Therefore, the dynamics of the three columns are in fact similar and may be described by similar mathematical models (Muresan et al., 2015). These models have been validated with partial data from the real plant in frequency domain multivariable context identification with the method described in (Ugryumova et al., 2015).

The model of the first column is given by:

$$\begin{pmatrix} p_{t1} \\ h_{CO1} \\ p_{b1} \end{pmatrix}(s) = \begin{pmatrix} \frac{-0.1111}{s^2+1.094s+0.08423}e^{-10s} & \frac{0.1152}{s^2+1.211s+0.2021}e^{-32s} & 0 \\ \frac{-0.001731}{s^2+0.1343s+0.001961}e^{-10s} & \frac{0.003846}{s^2+0.1547s+0.004357}e^{-8s} & \frac{-1.104}{s+0.1176} \\ \frac{-0.009918}{s^2+1.056s+0.07036}e^{-18s} & \frac{0.006288}{s^2+1.085s+0.09851}e^{-35s} & \frac{8.457}{s+0.9851} \end{pmatrix} \begin{pmatrix} W_1 \\ F_1 \\ P_{el1} \end{pmatrix}(s) \tag{1}$$

The model of the second column is given by:

$$\begin{pmatrix} p_{t2} \\ h_{CO2} \\ p_{b2} \end{pmatrix}(s) = \begin{pmatrix} \frac{-0.1111}{s^2+1.111s+0.1011}e^{-8s} & \frac{0.1152}{s^2+1.311s+0.3033}e^{-30s} & 0 \\ \frac{-0.001731}{s^2+0.13s+0.0022}e^{-8.5s} & \frac{0.003846}{s^2+0.15s+0.0044}e^{-7s} & \frac{-1.104}{s+0.12} \\ \frac{-0.009918}{s^2+1.06s+0.0784}e^{-16s} & \frac{0.006288}{s^2+1.105s+0.1225}e^{-30s} & \frac{8.457}{s+0.98} \end{pmatrix} \begin{pmatrix} W_2 \\ F_2 \\ P_{el2} \end{pmatrix}(s) \tag{2}$$

and the model of the third column is given by:

$$\begin{pmatrix} p_{t3} \\ h_{CO3} \\ p_{b3} \end{pmatrix}(s) = \begin{pmatrix} \frac{-0.1111}{s^2+1.131s+0.1213}e^{-7s} & \frac{0.1152}{s^2+1.361s+0.3538}e^{-24s} & 0 \\ \frac{-0.001731}{s^2+0.145s+0.003}e^{-6s} & \frac{0.003846}{s^2+0.17s+0.006}e^{-5s} & \frac{-1.104}{s+0.14} \\ \frac{-0.009918}{s^2+1.085s+0.0985}e^{-13s} & \frac{0.006288}{s^2+1.12s+0.133}e^{-27s} & \frac{8.457}{s+0.985} \end{pmatrix} \begin{pmatrix} W_3 \\ F_3 \\ P_{el3} \end{pmatrix}(s) \quad (3)$$

with manipulated variables the waste flow, feed-flow and electrical power supply in each column, and controlled variables: the top pressure, bottom pressure and liquid CO level in each column.

We have assumed simple models describing the interaction between the columns as:

$$\begin{aligned} h_{CO1}(s) &= \frac{1}{10s+1}W_2(s),\; h_{CO1}(s) = \frac{-1}{10s+1}F_2(s) \\ h_{CO2}(s) &= \frac{1}{10s+1}W_3(s),\; h_{CO2}(s) = \frac{-1}{7.5s+1}F_3(s) \\ h_{CO3}(s) &= \frac{-1}{6s+1}P_3(s) \end{aligned} \quad (4)$$

where P_3 is the product flow from the third column.

3. THE EPSAC APPROACH TO MULTIVARIABLE MPC

EPSAC stands for Extended Prediction Self-Adaptive Control and its pioneering ideas have been developed in the late 70s (De Keyser and Van Cauwenberghe, 1979), and published in early 80s. The methodology has been successfully applied in the last decades in several industrial (De Keyser and Van Cauwenberghe, 1980; De Keyser, 1997; Galvez et al., 2009). A comprehensive tutorial has been published in (De Keyser, 2003). A short summary will be given hereafter, for a 2x2 process; however, the matrix formulation can be easily adapted for nxn systems.

The basic equation for MIMO EPSAC for a 2x2 process is given by:

$$\begin{aligned} y_1(t) &= x_1(t) + n_1(t) \\ y_2(t) &= x_2(t) + n_2(t) \end{aligned} \quad (5)$$

where

$$\begin{aligned} x_1(t) &= f_1[x_1(t-1), x_1(t-2), ..., u_1(t-1), u_1(t-2), ...] \\ x_2(t) &= f_2[x_2(t-1), x_2(t-2), ..., u_2(t-1), u_2(t-2), ...] \end{aligned} \quad (6)$$

These functions depend on past inputs and past model outputs and can have any structure: linear, nonlinear, neural networks, etc. There exists also the variant where the past measured outputs of the process are used instead of past model outputs, for details see (De Keyser, 2003). In the remainder of this paper we will consider linear models.

The term in $n(t)$ denote the disturbance and modelling errors effects, modelled by coloured noise:

$$\begin{aligned} n_1(t) &= \frac{C_1(q^{-1})}{D_1(q^{-1})}e_1(t) \\ n_2(t) &= \frac{C_2(q^{-1})}{D_2(q^{-1})}e_2(t) \end{aligned} \quad (7)$$

with $e(t)$ white noise signals. The algorithm presented in detail in (De Keyser, 2003) introduces the concepts of base response and optimizing response:

$$\begin{aligned} y_1(t+k|t) &= y_{1Base}(t+k|t) + y_{1Opt}(t+k|t) \\ y_2(t+k|t) &= y_{2Base}(t+k|t) + y_{2Opt}(t+k|t) \end{aligned} \quad (8)$$

or in matrix format:

$$\begin{bmatrix} y_{1Opt}(t+1|t) \\ y_{1Opt}(t+2|t) \\ ... \\ ... \\ y_{1Opt}(t+N_2|t) \end{bmatrix} = \begin{bmatrix} h_1^{11} & 0 & 0 & ... & 0 \\ h_2^{11} & h_1^{11} & 0 & ... & 0 \\ ... & ... & ... & ... & ... \\ ... & ... & ... & ... & ... \\ h_{N_2}^{11} & h_{N_2-1}^{11} & h_{N_2-2}^{11} & ... & g_{N_2-N_u+1}^{11} \end{bmatrix} \begin{bmatrix} \delta u_1(t|t) \\ \delta u_1(t+1|t) \\ ... \\ ... \\ \delta u_1(t+N_u-1|t) \end{bmatrix} + \begin{bmatrix} h_1^{12} & 0 & 0 & ... & 0 \\ h_2^{12} & h_1^{12} & 0 & ... & 0 \\ ... & ... & ... & ... & ... \\ ... & ... & ... & ... & ... \\ h_{N_2}^{12} & h_{N_2-1}^{12} & h_{N_2-2}^{12} & ... & g_{N_2-N_u+1}^{12} \end{bmatrix} \begin{bmatrix} \delta u_2(t|t) \\ \delta u_2(t+1|t) \\ ... \\ ... \\ \delta u_2(t+N_u-1|t) \end{bmatrix} \quad (9)$$

In this equation, $y_{1Opt}(t+k|t)$ denotes the part in the predicted process output $y_1(t+k|t)$ coming from both optimizing control actions $\delta u_1(t+k|t)$ and $\delta u_2(t+k|t)$. In the special case of a 2x2 system, we need to have 4 impulse responses, i.e. from each input j to each output i, with notation $\{h_1^{ij}, h_2^{ij}, h_3^{ij}, ...\}$. From (9), a similar relation can be derived for $y_{2Opt}(t+k|t)$. Notice that the prediction horizons N_2 could be different for the two outputs, whereas the control horizons N_u could be different for the two inputs.

The key equation for MIMO EPSAC is then:

$$\begin{aligned} \mathbf{Y_1} &= \mathbf{\bar{Y}_1} + \mathbf{G_{11}} \cdot \mathbf{U_1} + \mathbf{G_{12}} \cdot \mathbf{U_2} \\ \mathbf{Y_2} &= \mathbf{\bar{Y}_2} + \mathbf{G_{21}} \cdot \mathbf{U_1} + \mathbf{G_{22}} \cdot \mathbf{U_2} \end{aligned} \quad (10)$$

3.1 Solidary Control

This strategy is ideally represented in figure 2. Notice there is cooperation between all control signals.

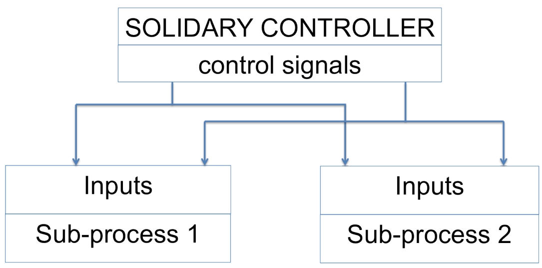

Fig. 2. Conceptual representation of solidary EPSAC.

The cost function is given by:

$$\sum_{k=N_1}^{N_2} [r_1(t+k|t) - y_1(t+k|t)]^2 + \sum_{k=N_1}^{N_2} [r_2(t+k|t) - y_2(t+k|t)]^2 \quad (11)$$

with r_j denoting reference signals for all j controlled outputs and subject to $u_1(t+k|t) = u_1(t+N_u-1|t)$ and to $u_2(t+k|t) = u_2(t+N_u-1|t)$ for $k \geq N_u$. which is also valid for the case when the number of inputs differs from the number of outputs. In (11), the predicted control errors summed over all process outputs are minimized. In practice, this implies that some variables may deliberately allow more errors to help other variables reach the setpoint in order to minimize the global cost. Hence the name, *solidary control*.

If one re-writes (11) in matrix format and transforms in the standard quadratic cost index:

$$\mathbf{J}(\mathbf{U}) = \mathbf{U}^\mathbf{T}\mathbf{H}\mathbf{U} + 2\mathbf{f}^\mathbf{T}\mathbf{U} + c \tag{12}$$

it follows that:

$$\begin{aligned}\mathbf{H} &= \mathbf{G_1^T G_1} + \mathbf{G_2^T G_2}\\ \mathbf{f} &= -\left[\mathbf{G_1^T}(\mathbf{R_1} - \bar{\mathbf{Y}}_\mathbf{1}) + \mathbf{G_2^T}(\mathbf{R_2} - \bar{\mathbf{Y}}_\mathbf{2}\right]\\ c &= (\mathbf{R_1} - \bar{\mathbf{Y}}_\mathbf{1})^\mathbf{T}(\mathbf{R_1} - \bar{\mathbf{Y}}_\mathbf{1}) + (\mathbf{R_1} - \bar{\mathbf{Y}}_\mathbf{1})^\mathbf{T}(\mathbf{R_1} - \bar{\mathbf{Y}}_\mathbf{1})\end{aligned} \tag{13}$$

with $G_1 = [G_{11} \;\; G_{12}]$ and $G_2 = [G_{21} \;\; G_{22}]$. In the situation there are no constraints active, the exact solution is given by $\mathbf{U}^* = -\mathbf{H}^{-1}\mathbf{f}$, as:

$$\begin{aligned}\mathbf{U}^* = &\left[\mathbf{G_1^T G_1} + \mathbf{G2^T G_2}\right]^{-1} \cdot\\ &\left[\mathbf{G_1^T}(\mathbf{R_1} - \bar{\mathbf{Y}}_\mathbf{1}) + \mathbf{G_2^T}(\mathbf{R_2} - \bar{\mathbf{Y}}_\mathbf{2})\right]\end{aligned} \tag{14}$$

3.2 Selfish Control

This strategy is ideally represented in figure 3. Here it is crucial the choice of the pairings as the most important signal is chosen for each local controller. The other input signals are treated as known disturbances. As the name suggests, the local controller only wants to minimize errors on its specific output.

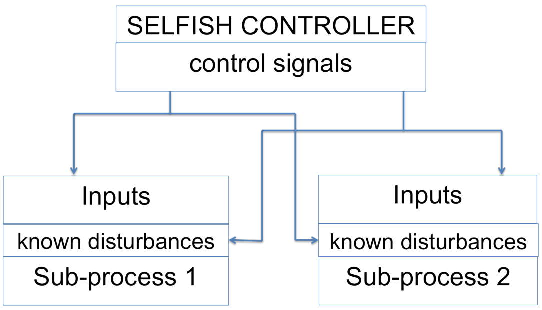

Fig. 3. Conceptual representation of selfish EPSAC.

Following the same reasoning line as for solidary control, we have that the optimal control vector $\mathbf{U_1^*}$ is found minimizing:

$$\sum_{k=N_1}^{N_2} \left[r_1(t+k|t) - y_1(t+k|t)\right]^2 \tag{15}$$

subject to $u_1(t+k|t) = u_1(t+N_u-1|t)$ for $k \geq N_u$; and that equivalently, the optimal control vector $\mathbf{U_2^*}$ is found minimizing:

$$\sum_{k=N_1}^{N_2} \left[r_2(t+k|t) - y_2(t+k|t)\right]^2 \tag{16}$$

subject to $u_2(t+k|t) = u_2(t+N_u-1|t)$ for $k \geq N_u$. This objective is applicable only if the number of manipulated input variables is the same as the number of controlled output variables. This cost function minimizes the individual control error of each variable separately, but taking into account the effect of all actions from other variables as well. In this context, the minimization is in competition with the other variables, hence the name *selfish control*.

Applying the same quadratic formulation as in (12), it follows that:

$$\begin{aligned}\mathbf{H_1} &= \mathbf{G_{11}^T G_{11}}\\ \mathbf{f_1} &= -\mathbf{G_{11}^T}(\mathbf{R_1} - \bar{\mathbf{Y}}_\mathbf{1} - \mathbf{G_{12}U_2})\\ \mathbf{c} &= (\mathbf{R_1} - \bar{\mathbf{Y}}_\mathbf{1} - \mathbf{G_{12}U_2})^\mathbf{T}(\mathbf{R_1} - \bar{\mathbf{Y}}_\mathbf{1} - \mathbf{G_{12}U_2})\end{aligned} \tag{17}$$

whereas minimization with respect to U_1 leads to the explicit solution:

$$\mathbf{U_1^*} = \left[\mathbf{G_{11}^T G_{11}}\right]^{-1}\left[\mathbf{G_{11}^T}(\mathbf{R_1} - \bar{\mathbf{Y}}_\mathbf{1} - \mathbf{G_{12}U_2})\right] \tag{18}$$

Similarly, one obtains for U_2 the explicit solution:

$$\mathbf{U_2^*} = \left[\mathbf{G_{22}^T G_{22}}\right]^{-1}\left[\mathbf{G_{22}^T}(\mathbf{R_1} - \bar{\mathbf{Y}}_\mathbf{1} - \mathbf{G_{21}U_1})\right] \tag{19}$$

In these relations, notice the presence of interaction terms, which indicates this is a multivariable strategy and not a single input single output formulation. We reach a SISO approach if $G_{12} = 0$ in (18), and $G_{21} = 0$ in (19).

In matrix formulation we have that:

$$\mathbf{U}^* = \begin{bmatrix}\mathbf{G_{11}^T G_1}\\ \mathbf{G_{22}^T G_2}\end{bmatrix}^{-1}\begin{bmatrix}\mathbf{G_{11}^T}(\mathbf{R_1} - \bar{\mathbf{Y}}_\mathbf{1})\\ \mathbf{G_{22}^T}(\mathbf{R_2} - \bar{\mathbf{Y}}_\mathbf{2})\end{bmatrix} \tag{20}$$

with $G_1 = [G_{11} \;\; G_{12}]$ and $G_2 = [G_{21} \;\; G_{22}]$.

When constraints are not active, both solidary and selfish strategies give nearly identical closed loop performance.

3.3 Dealing with (Variable) Time Delays

The complexity of the prediction procedure is of a higher order for systems with (variable) time delay than for those with constant time delay. For a system with time delay, changes in the controlled variable are noticeable once the time delay has passed. Therefore, in order to find the optimal control sequence only output predictions occurring after the time delay should be taken in the cost function. This means that the minimum costing horizon N_1 should be equal to the time delay. For systems with constant time delay this is easy to do. Then the maximum prediction horizon N_2 can be set to an appropriate value that ensures a stable and robust response and the control loop can be operated with fixed controller parameters.

For a variable time delay however, the value of N_1 (and thus also N_2) varies with the dead-time index. In (Sbarciog et al., 2008) the structure of the process model is exploited to design a predictive controller with constant design parameters. The principle is illustrated in figure 4.

Figure 4 depicts the Smith-Predictor like EPSAC formulation for processes with variable time delays (Normey-Rico, 2007). At each sampling instant, the delay-free model output $x(t)$, resulting from the process dynamics only, is calculated using the stored values $[x(t1), ..., u(t1), ...]$. At the same sampling instant, the variable time delay is estimated/computed. Once the delay value in samples N_d

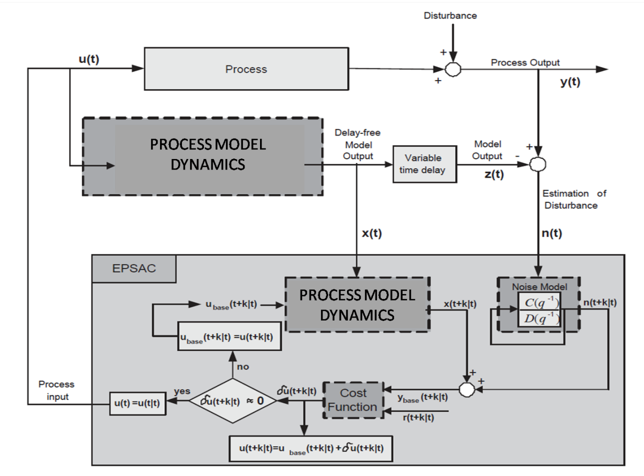

Fig. 4. Smith-Predictor like EPSAC formulation for processes with different time delays or variable time delays.

is known, $x(tN_d)$ can be selected out of the stored x-values, such that $z(t) = x(tN_d)$.

In this way, the prediction procedure is thoroughly simplified, resulting in a Smith predictor-like scheme, with separation of the tank and tube dynamics on one hand and the varying time delay on the other hand. In such approach the minimum prediction horizon is no longer varying and obviously equal to one. Hence, the maximum prediction horizon is also constant.

4. RESULTS AND DISCUSSION

This section presents the results of the EPSAC tests on the train of distillation columns afore mentioned. The sampling period is 1 minute, and all related designs are reported in samples. The model for prediction contains only the relations between the manipulated inputs: feed flow in the first, second and third column respectively, and the controlled outputs: carbon isotope in first, second and third column. Information upon reflux from third to second column and from second to first column is also used for prediction.

The control scenario is as follows: follow the desired trajectory in the output of the third column, while maintaining the other outputs around their operating point. All variables have been scales to work between $\pm 100\%$ and normalized operating point is denoted by 0.

Constraints on the input-output variables are set as follows:

$$\begin{aligned} 10\% \leq U_1, U_2, U_3 \leq 50\% \\ -100\% \leq Y_1, Y_2, Y_3 \leq 100\% \end{aligned} \quad (21)$$

and a limit on the variation of the control effort between sampling period of 10%.

The prediction horizon N_2 has been set to 70 samples for all manipulated inputs, and a constant delay of 7 samples has been introduced in the prediction. The control horizon N_u is one sample. Notice that there are modelling errors present in terms of time delay, i.e. the assumed constant delay of 7 samples for prediction purposes is obviously not

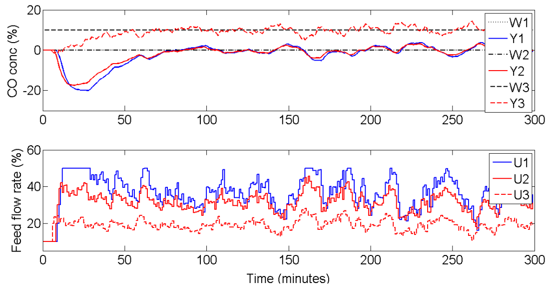

Fig. 5. Selfish EPSAC for train of distillation columns: controlled percent carbon isotope (top) and manipulated feed flows (bottom).

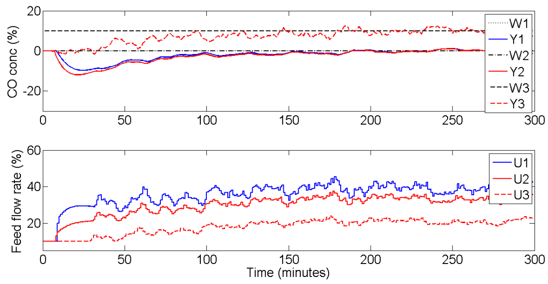

Fig. 6. Solidary EPSAC for train of distillation columns: controlled percent carbon isotope (top) and manipulated feed flows (bottom).

the same as the time delay in the real plant, with errors varying between 450% and 10%. A real-time estimation of the delay is possible to be implemented on top of this control architecture. For instance, using correlation function analysis from signals measured online and delay estimated using a moving window.

Figure 5 presents the result for *selfish* EPSAC strategy, while figure 6 depicts the result for *solidary* EPSAC strategy. Both results indicate good performance in closed loop. As expected, when active constraints are present, these strategies differ in performance. The solidary approach is less aggressive, more robust, trying to bring all players to their desired values. By contrast, the selfish approach is has faster tracking at the cost of destabilizing more the other players, as each player is eager to reach the desired value as fast as possible.

A more reasonable constraint interval has values centered around the operating point where the models have been identified. The next test has the following constraints:

$$\begin{aligned} -10\% \leq U_1, U_2, U_3 \leq 30\% \\ -100\% \leq Y_1, Y_2, Y_3 \leq 100\% \end{aligned} \quad (22)$$

and a limit on the variation of the control effort between sampling period of 10%.

Figure 7 presents the result for *selfish* EPSAC strategy, while figure 8 depicts the result for *solidary* EPSAC strategy. Again, we observe that the outputs follow the reference trajectory within the constrained interval. The same conclusion holds that selfish control has better performance than solidary control at the price of a more aggressive control effort. The fact that now the constraints

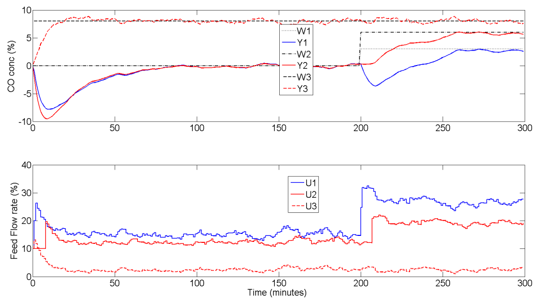

Fig. 7. New constraints: selfish EPSAC for train of distillation columns: controlled percent carbon isotope (top) and manipulated feed flows (bottom).

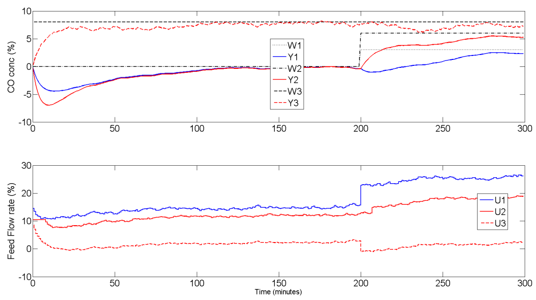

Fig. 8. New constraints: solidary EPSAC for train of distillation columns: controlled percent carbon isotope (top) and manipulated feed flows (bottom).

are defined around the operating point leads to improved overall performance with 30% in the settling time.

5. CONCLUSION

This work presented an important step in control of a train of distillation column for ^{13}C carbon isotope production. A model based predictive control strategy has been employed, input-output constrained, on a simplified linear model of the cascaded columns. Next steps in this work are the inclusion of variable time delays (due to changes in the operating points) and robustness analysis with respect to model uncertainty.

REFERENCES

Axente, D., Abrudean, M., and Gligan, M. (1994). *Isotope Separation $^{15}N^{18}O^{10}B^{13}C$ by isotopic exchange*. Casa Cartii de Stiinta (in Romanian), Cluj Napoca.

Bisgaard, T., Huusom, J., and Abildskov, J. (2015). Modeling and analysis of conventional and heat-integrated distillation columns. *AIChe J*, 61(-), 4251–4263.

De Keyser, R. (1997). Improved mould level control in a continuous steel casting line. *Control Engineering Practice*, 5(2), 231–237.

De Keyser, R. (2003). Model based predictive control for linear systems. In *UNESCO Encyclopaedia of Life Support Systems, CONTROL SYSTEMS, ROBOTICS AND AUTOMATION*, volume XI, chapter Article contribution 6.43.16.1, 30 pages. Eolss Publishers Co Ltd, Oxford.

De Keyser, R. and Van Cauwenberghe, A. (1979). A self-tuning predictor as operator guide. *In: R. Isermann (Ed.), Identification and System Parameter Estimation*, 1249–1256.

De Keyser, R. and Van Cauwenberghe, A. (1980). Self-tuning load-following control of a nuclear power plant. *In: J.F. Herbst (Ed.), Automatic Control in Power Generation, Distribution and Protection, Pergamon Press Oxford*, 227–234.

Galvez, M., De Keyser, R., and Ionescu, C. (2009). Nonlinear predictive control with dead-time compensator: Application to a solar power plant. *Solar Energy*, 83(-), 743–752.

Luyben, W. (2013). Control of a train of distillation columns for the separation of natural gas liquid. *Ind Eng Chem Res*, 52(31), 10741–10753.

Muntean, I., Unguresan, M., Savu, A., and Abrudean, M. (2012). Modeling and composition estimation of an isotopic distillation column. In *IEEE International Conference on Automation Quality Testing and Robotics*. IEEE, Cluj, Romania, 24-27 May. 109–113.

Muresan, C., Dulf, E., and Both, R. (2015). Comparative analysis of different control strategies for a train of cryogenic ^{13}c separation columns. *Chem Eng Tech*, 38(4), 619–631.

Normey-Rico, J. (2007). *Control of Dead-Time processes*. Springer, London.

Pop, C., Festila, C., and Dulf, E. (2010). Optimal control of the carbon isotopes cryogenic separation process. *Chemical and Biochemical Engineering Quarterly*, 24(3), 301–307.

Pop, C., Ionescu, C., and De Keyser, R. (2012). Time delay compensation for the secondary processes in a multivariable carbon isotope separation unit. *Chemical Engineering Science*, 80(-), 205–218.

Sbarciog, M., De Keyser, R., Cristea, S., and De Prada, C. (2008). Nonlinear predictive control of processes with variable time delay. a temperature control case study. In *IEEE International Conference on Control Applications*. IEEE, San Antonio, CA Date: SEP 03-05. 601–606.

Skogestad, S. (1997). Dynamics and control of distillation columns - a critical survey. *10.4173/mic.1997.3.1*, 18(3), 177–217.

Ugryumova, D., Pintelon, R., and Schoukens, J. (2015). Frequency response matrix estimation from missing input output data. *IEEE Trans Instr Meas*, 64(11), 3124 – 3136.